Available online at www.sciencedirect.com
SCIENCE DIRECT®

Journal of the European Ceramic Society 23 (2003) 2857–2866
www.elsevier.com/locate/jeurceramsoc

Influence of fibre–matrix interface on the fracture behaviour of carbon-carbon composites

C. Blanco*, E. Casal, M. Granda, R. Menéndez

Instituto Nacional del Carbón CSIC, Apdo. 73, 33080-Oviedo, Spain

Abstract

This paper studies the fracture behaviour of unidirectional carbon fibre reinforced carbon matrix composites and its relation with the type of fibre–matrix interface developed in the composite. Model unidirectional carbon–carbon composites were prepared using the same type of fibre and different pitches as matrix precursors. These included both commercial pitches and synthesized in the laboratory ones. The chemical composition of the matrix precursor determined the type of microstructure developed in the composite, this microstructure seems to govern the fibre-matrix bonding and in turn controls the fracture behaviour of the composite. In general, a matrix texture of mosaic (small size) seems to yield a good fibre-matrix bonding, making the materials to have higher interlaminar shear strength but having at the same time brittle fracture behaviour. On the other hand, composites where larger textures were developed in the matrix seem to have a poorer fibre-matrix bonding. This made the composites to have lower strength, but it allowed debonding of fibre and matrix during fracture. As a result, these materials showed pseudo-plastic failure behaviour. Other examples of both types of fracture behaviour associated with the change in microstructure and fibre–matrix interface are discussed.

Keywords: Carbon; Composites; Interfaces; Mechanical properties; Microstructure-final

1. Introduction

Carbon fibre reinforced-carbon matrix composites are unique materials that can have high specific thermal and mechanical properties at elevated temperatures. They are widely used in high performance applications in the military and aerospace industry and, in considerable quantities, as friction elements in aircraft braking systems.[1,2] However, the main drawback in the use of carbon–carbon composites in conventional applications is their high costs derived from the complexity and length of the fabrication processes.[2] Despite they have been developed decades ago, there is still a need for a better understanding of the factors controlling their thermal and mechanical properties in order to optimise their processing and better predict their properties.

The physical properties and fracture behaviour of carbon–carbon composites are determined by the type of architecture of the fibres and the microstructure of the supporting matrix. The microstructure of a carbon–carbon composite may be described in terms of its porosity, interfaces and texture, and it largely depends on the chemical composition and physical properties of the matrix precursor, as well as on the processing conditions.[3,4] Two main types of matrix precursors are currently used in the preparation of carbon–carbon composites by liquid impregnation: resins and pitches. The latter offers great possibilities because of the wide range of pitches with different characteristics available, their relatively low price and high carbon yield and, specially, because of their ability to generate graphitisable matrices. The main sources of pitch are coal and petroleum, each one having different chemical composition. Coal-derived pitches are more aromatic, with compounds of higher condensation degree and they contain carbonaceous particles (<1 μm) called primary quinoline insolubles (QI), which are generated during the coke oven operation and remain in the pitch.

In addition to the individual characteristics of fibre and matrix, both components may undergo mutually dependent structural changes during fabrication of the composite. Thus fibre–matrix interactions may control the development of the main structural features, and

* Corresponding author. Tel.: +34-985-11-90-90; fax: +34-985-29-76-62.
E-mail address: clara@incar.csic.es (C. Blanco).

0955-2219/03/$ - see front matter © 2003 Elsevier Ltd. All rights reserved.
doi:10.1016/S0955-2219(03)00298-X

have also been recognized as a key factor to control the efficiency and effectiveness of the liquid impregnation densification stage.[5] The knowledge of the composition of matrix precursors, their behaviour during processing and the effect of the fibre as a result of their mutual interactions may be of special relevance for designing composites with specific microstructures.[5]

This paper studies the fracture behaviour of unidirectional carbon–carbon composites and its relation with the type of fibre–matrix interface developed in the composite. Model unidirectional carbon–carbon composites were prepared using the same type of fibre and different matrix precursors, both commercial and synthesized in the laboratory. Examples of both brittle and pseudo-plastic fracture behaviour are presented and discussed in terms of the microstructure of the composite and the characteristics of the matrix precursor.

2. Experimental

2.1. Raw materials

The carbon fibres used for the preparation of model unidirectional carbon–carbon composites were high-strength, high-strain polyacrilonitrile (PAN)-based fibres ASA-12K supplied by Hercules Aerospace, Madrid. The fibre diameter is 7 μm and its surface has been treated and sized to improve its interlaminar shear properties.

A variety of carbon matrices were used for the preparation of the carbon composites. Initially, three pitches of different origin were used as matrix precursors. These were a binder coal-tar pitch, a liquefaction pitch and a petroleum pitch. Further details on the characteristics of these pitches are described elsewhere.[6] Composites obtained using these pitches were labelled C-BP, C-LP and C-PP, respectively. An additional composite prepared using a synthetic pitch derived from anthracene oil after an air-blowing treatment was also used for comparison purposes. As primary quinoline insoluble particles present in coal-tar pitches improve the strength of pitch-based cokes, a second set of composites was prepared using pitches with different primary quinoline insoluble content. In order to keep a low number of variables, the same raw pitch was used to prepare synthetic pitches with 0, 11 and 50 wt.% primary quinoline insoluble content. The resultant composites were accordingly labelled C-QI0, C-QI11 and C-QI50, respectively.

Finally, the role of fibre–matrix interface on the mechanical behaviour of the composites was studied in a series of composites that were submitted to successive densification cycles, from 0 to 5, using a binder coal-tar pitch as impregnating agent. The resultant composites were labelled according to the number of densification cycles used, C-DN0 to C-DN5, respectively.

2.2. Preparation of composites

Model unidirectional carbon fibre reinforced-carbon matrix composites were prepared by the wet-winding technique, using a procedure previously described,[6] which is similar to that used by Ahearn and Rand.[7] Carbon fibre tows were impregnated with a solution/suspension of pitch in tetrahydrofuran (THF) in a 1:1 concentration and then wound on a rotating plate. THF acts as a support agent of the pitch, both its soluble and its insoluble parts being deposited on the fibre during the wet winding. Ultrasonic was used to obtain a good homogenisation and to avoid pitch segregation during the impregnation processes. THF was removed at 60 °C under vacuum. The temperature was then increased up to 10 °C below the softening point of the pitch and maintained for 10 h. During this process, the prepreg was placed between two metallic plates to prevent deformation. Laminates of 170×70 mm were cut and consolidated to ca. 4 mm thickness.

Samples of 130×60 mm were also cut and heated at 5 °C min^{-1} to temperatures between 415 °C and 550 °C for 30 to 60 min, under a continuous flow of nitrogen. Based on previous studies,[8] 3 MPa uniaxial mechanical pressure was applied at different temperatures depending on the nature of the pitch used as carbon matrix precursor. In a subsequent pyrolysis step, a portion of 110×49 mm of each composite was placed in a graphite mould and carbonised in a horizontal furnace, under a continuous flow of argon (65 ml min^{-1}), at a heating rate of 1 °C min^{-1} to 1100 °C, and this temperature maintained for 30 min, at atmospheric pressure. After carbonisation, the composites were cooled down to room temperature at 1 °C min^{-1}.

2.3. Characterisation of composites

2.3.1. Mechanical properties

The flexural strength of the composites was determined by the three-point bending test according to ASTM D790-86 standard. Samples of 10 mm width were cut in the fibre direction (flexural 0°) and then tested in the three-point bend rig over a span of 100 mm, between an 8 mm diameter supporting roller and an 8 mm diameter loading roller. The machine cross-head speed used was 2.6 mm min^{-1}. The results are quoted as the mean of values from five samples of each composite.

The interlaminar shear strength (ILSS) test was carried out on the composites according to standard procedures (ISO 4585 and ASTM D2344-84 standards). Samples of 5 mm width were cut in the fibre direction and tested in a three-point bending rig over a span of 8 mm, between a 3 mm diameter supporting roller and a 6 mm diameter loading roller. The machine cross-head speed used was 1 mm min^{-1}. The results were quoted as the mean of the values from eight samples of each composite.

2.3.2. Optical microscopy

Samples of composites for optical microscopy examination were cut, embedded in epoxy resin and polished following a procedure described elsewhere.[9] Optical microscopy analyses were made using a microscope with oil immersion 20×, 50× and 100× objectives in conjunction with a swift automatic point-counter. The microscope included a $1-\lambda$ retarder plate to record the optical texture of the anisotropic matrix. The analysis of each composite involved the identification of fibres, matrix and pores located at the intersection of graticulate cross-hair. Moreover, cracks (intramatrix and interface located) were also identified. Quantification was achieved by recording 500 individual determinations using an interpoint and interline distance of 0.5 mm. The number of counts recorded was converted to a proportion by volume of the total. The optical texture of the matrix was also characterised.[10]

2.3.3. Scanning electron microscopy

The orientation of constituent lamellar structures of the matrix with respect to the fibres was qualitatively determined by scanning electron microscopy (SEM) of polished cross-sections of the composites after etching with a chromic acid solution for 4 h.[11] Fibre–matrix adhesion and fracture behaviour after mechanical testing was monitored by SEM.

3. Results and discussion

3.1. Influence of matrix precursor

One of the main advantages that the use of pitch as matrix precursor offers is the variety of microstructures in the composite matrix that can be generated by the careful selection of precursors and preparation conditions, thus affecting the mechanical behaviour of the composite. Three pitches of rather different characteristics were selected as matrix precursors and the resultant composites studied. These matrix precursors behaved differently on carbonisation, giving rise to carbon matrices that show a variety of microstructures.[10] This is shown in Fig. 1, which corresponds to optical

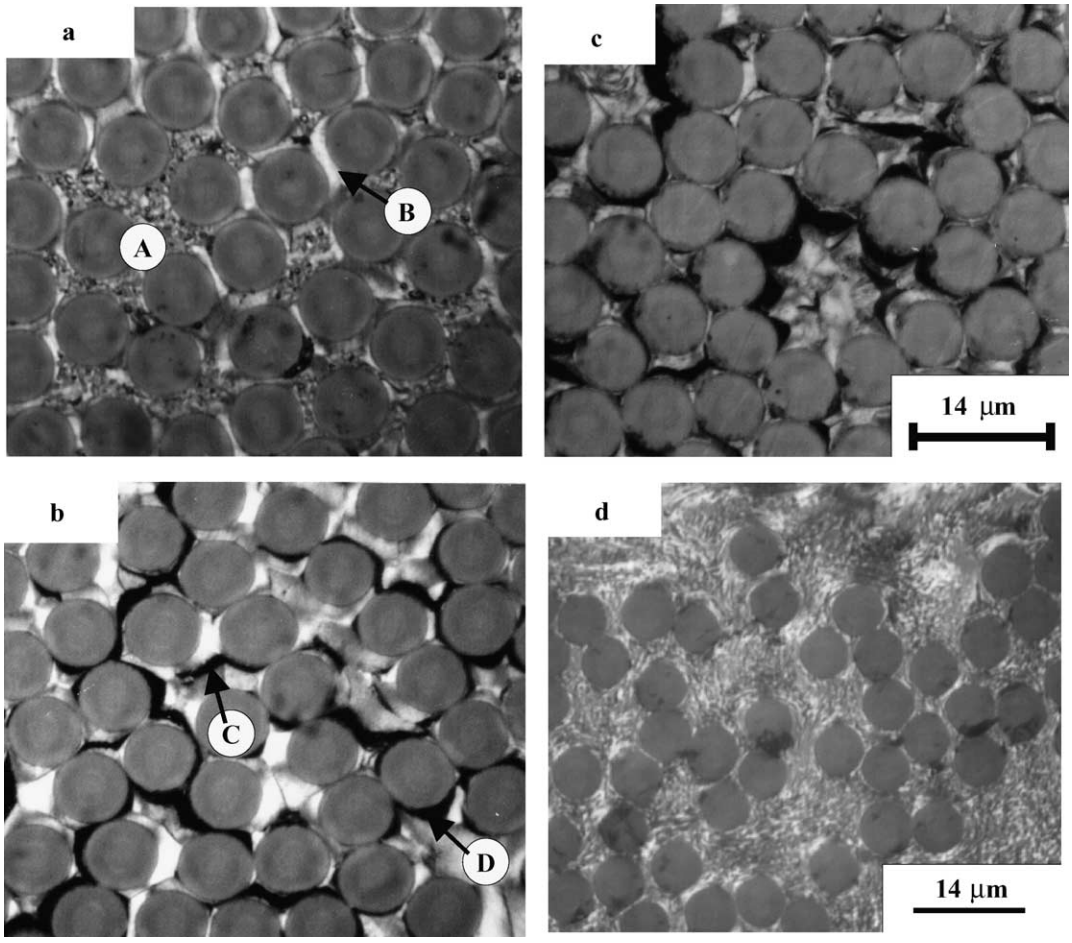

Fig. 1. Optical micrographs showing the different texture of the matrix in composites: (a) C-BP (b) C-LP, (c) C-PP and (d) C-AA. Mosaics (position A) and domains (position B) are combined in C-BP. C-LP and C-PP are mainly formed of domains and intramatrix cracks (position C) and cracks at the fibre–matrix interface are also observed. Mainly mosaics are observed in C-AA.

micrographs of polished surfaces of the composites. In the case of the binder pitch (Fig. 1a), two different microstructures in the matrix are observed. One is of smaller size (mosaics, Position A), and the other one, of larger size (domains, Position B), is normally observed surrounding the fibres. This is because this pitch contains small solid carbonaceous particles (primary quinoline insolubles, QI) that tend to form clusters, giving microstructures of small size. Other components of the precursor are able to develop anisotropic structures of larger size (domains), which in the case of carbon–carbon composites tend to orientate around the fibres.[12] On the other hand, matrix in composites obtained from less aromatic pitches, such as the petroleum and the liquefaction ones (Fig. 1b and c), is mainly forming domains, again oriented around the fibres. The development of these microstructures is related to the lower viscosity of these pitches, which at the same time makes the volume fraction of fibres to be higher for composite C-PP (Table 1), as part of the matrix precursor exudates during processing. Composite C-BP also showed the highest density of the three composites, 1.59 vs. 1.46 g cm^{-3} obtained for composite C-PP. Different to the composite obtained from the coal-tar pitch (Fig. 1a), these two composites show shrinkage cracks located within the matrix (Fig. 1b, position C) and also at the fibre–matrix interface (Fig. 1b, position D). This is a typical feature of matrices that form large domains, as there is a greater difference of shrinkage between matrix and fibres on carbonisation that causes debonding of fibre and matrix at the interfaces.[13] The difference in texture, which suggests the development of a different type of interface, is also clearly distinguished in the SEM images presented in Fig. 2. The matrix in the composite obtained from the coal-tar pitch (Fig. 2a) shows areas of smaller size, which resemble particles (primary quinoline insolubles) and do not show debonding between fibre and matrix in a great extent. However, the regions where larger oriented structures were developed, do show a higher degree of debonding between fibre and matrix. In the case of the composite obtained with the petroleum pitch (Fig. 2b), the larger texture in the matrix is clearly observed, in agreement with the optical microscopy results. Also, debonding becomes the dominant feature of this composite at the fibre–matrix interface. Debonding cracks represent about 0.4 vol.% of the composite obtained from the coal tar pitch, while they are 2.6 and 6 vol.% in composites obtained from the liquefaction and petroleum pitch, respectively, as determined by optical microscopy.

The microstructures developed in the composites seem to play an important role in the mechanical properties of these materials. The composite obtained from the coal-tar pitch had the highest interlaminar shear strength of the three composites studied, 22.9 MPa, while it decreased as the degree of debonding increased in the composites, with values of 17.2 and 13.4 MPa for composites obtained from the liquefaction and petroleum pitches, respectively. Also, the type of interface developed in the composites seems to determine the failure mode of the composite (Fig. 3). Composites which microstructure suggests a weak

Table 1
Main properties of composites prepared using different commercial pitches as matrix precursors

Composite	V_f	d	P	$P_{f/m}$	ILSS
C-BP	61	1.59	10.6	0.4	22.9
C-LP	58	1.50	18.8	2.6	17.2
C-PP	72	1.46	13.8	6	13.5

V_f, volume fraction of fibres (vol.%); d, bulk density (g cm^{-3}); P, porosity (vol.%); $P_{f/m}$, fibre/matrix debonding cracks (vol.%); ILSS, interlaminar shear strength (MPa).

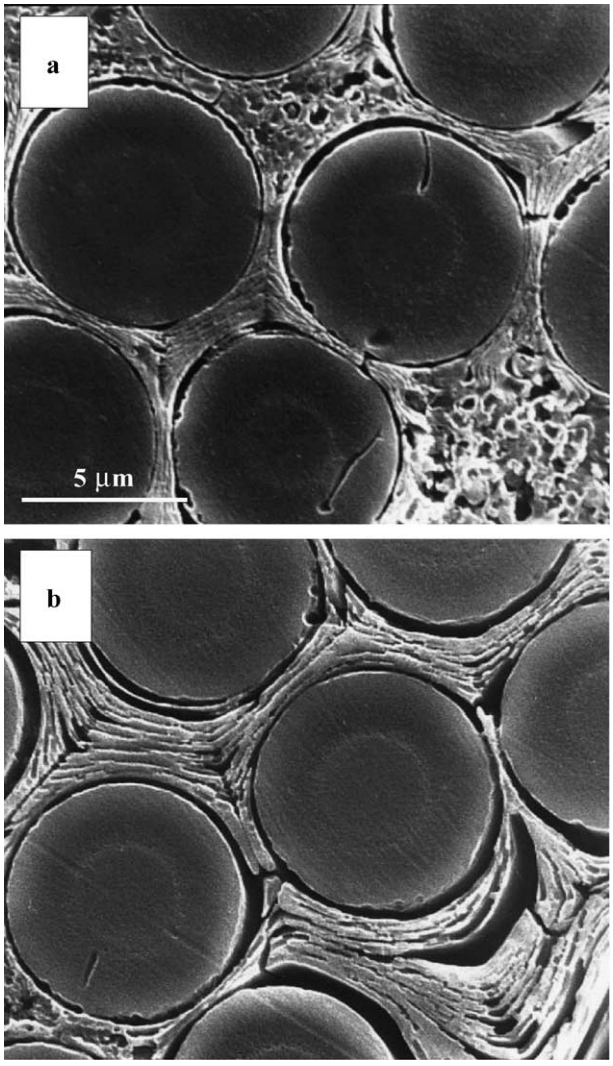

Fig. 2. SEM micrographs of composites: (a) C-BP and (b) C-PP, illustrating their different texture and interface developed, with debonding between fibre and matrix being more evident for C-PP.

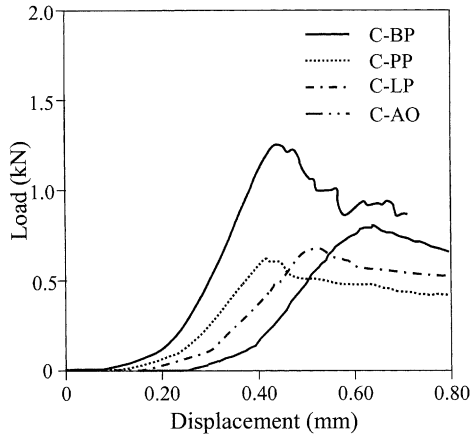

Fig. 3. Load–displacement curves of composites obtained with different matrix precursors. Composites C-LP and C-PP show pseudo-plastic fracture behaviour while C-BP exhibits a more brittle type of fracture.

interface normally yield pseudo-plastic fracture behaviour due to debonding of fibre and matrix, as occurs with composites C-LP and C-PP. On the other hand, composites that seem to have a stronger interface, like composite C-BP, exhibit a more brittle type of fracture behaviour. It is worth mentioning, however, that there are cases in which the materials do not behave as expected. This is the case of the composite obtained with the synthetic pitch derived from anthracene oil, which shows a texture of domains oriented around the fibres, but at the same time it seems to have a strong fibre–matrix adhesion, as suggested by the lack of cracks at the interface (Fig. 1d). Also unusual is the load-displacement curve obtained for this composite, which shows pseudo-plastic fracture behaviour despite the good fibre-matrix adhesion presumed for the composite (Fig. 3).

3.2. Effect of solid particles present in the matrix

It is generally accepted that the presence of primary quinoline insolubles in coal-tar pitches governs the development of mesophase and therefore, the final microstructure of the carbon materials resultant after carbonisation, in particular in the carbon matrices generated when these pitches are used as matrix precursors in carbon-carbon composites. The influence of primary quinoline insolubles on the microstructure and ultimately on the mechanical behaviour of carbon–carbon composites was studied in a series of model unidirectional composites made with the same PAN-based fibres and matrices obtained from the same pitch but containing different quinoline insolubles. The optical texture of these composites is shown in Fig. 4. When a matrix precursor free of quinoline insolubles is used (Fig. 4a), the matrix in the composite shows mainly domains, preferentially oriented around the fibres. Debonding cracks at the fibre–matrix interfaces are also observed. As the quinoline insoluble content increases (Fig. 4b), the contribution of mosaics to the microstructure of the matrix is more evident. The matrix is now formed by both mosaics and domains, the latter oriented around the fibres. Less debonding is observed in these composites. Finally, when the primary quinoline insoluble content is extremely high (Fig. 4c), the texture of the matrix is only formed by mosaics, no apparent debonding being observed. The clusters of QI particles do not show a preferential order around the fibres. It is noticeable that these clusters tend to disturb the spatial distribution of the fibres in the composite, causing the distribution of fibres to be irregular. This phenomenon is especially present in the composite from the residue, where the distribution of fibres is very irregular.

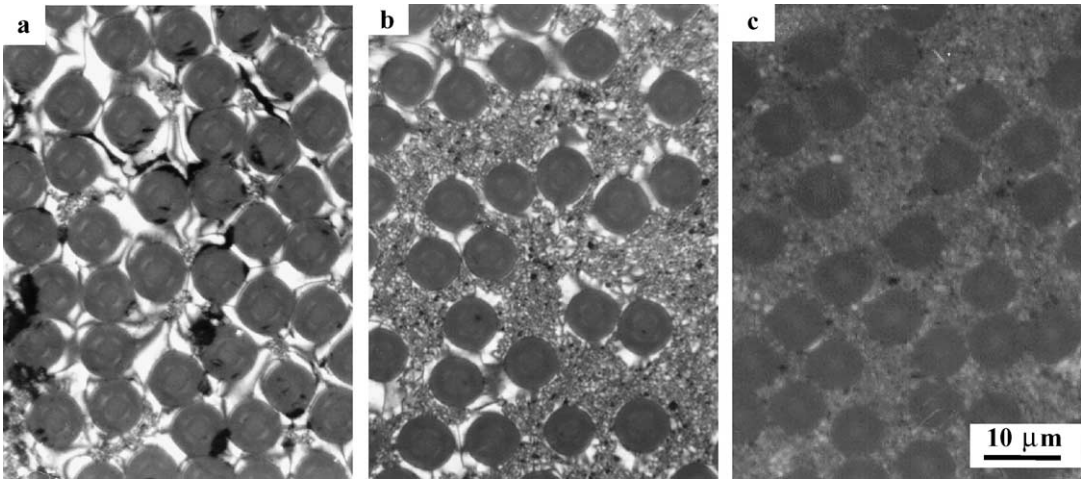

Fig. 4. Optical micrographs of composites: (a) C-QI0, (b) C-QI11 and (c) C-QI50. The higher the IQ content, the higher contribution of mosaics to the microstructure of the matrix and less debonding of fibre and matrix is observed.

These results indicate that the presence of QI clusters cause a reduction in the contraction of the matrix during carbonisation. A similar effect was described for the addition of carbon particles (carbon black) to the precursors.[14] These features are clearly observed in the SEM images shown in Fig. 5. In C-QI0 (Fig. 5a), the absence of QI leads to the formation of microcracks at the fibre–matrix interface, resultant from the contraction of the large crystalline structures during carbonisation. As the QI content increases (Fig. 5b), the number of microcracks at the interface decreases. Also, the volume fraction of matrix increases with increasing the QI content of the matrix (Table 2), probably due to the higher viscosity of the pitches containing higher QI, which limits exudation of the matrix during processing.

The fracture of C-QI0 and C-QI11 occurred by delamination, while C-QI50 failed on flexion, a fact that influences the dispersion of the data obtained. The values calculated for this composite are, therefore, not representative of the interlaminar shear strength, which must be significantly higher. Fig. 6 represents the load–displacement curves obtained from interlaminar shear testing. Although the QI content is not the only characteristic that varies from one composite to another, the comparison between the composites studied suggests that the presence of QI particles enhance the strength of the fibre–matrix bonding, resulting in an increase in the shear strength (from 24.9 MPa for composite C-QI0 to higher than 35.9 MPa for composite C-QI50), but at the same time leading to a more brittle behaviour. The mode of failure also changed with the presence of QI (Fig. 6). Composite C-QI0 shows a classical multiple fracture mode of failure leading to relative movement of the two phases as the load is transferred to the fibres. As observed by SEM (Fig. 7a), there is debonding which allows some fibre pullout, probably as a consequence of a poorer matrix–fibre interface. On the other hand, composite C-QI11 (Fig. 7b) failed in a totally brittle, catastrophic manner; fracture was preceded by linear, elastic behaviour up to a maximum stress, as illustrated in Fig. 6. It is likely that a stronger fibre–matrix interface of this composite increases load transfer to the fibre, this increasing the overall strength of the composite and causes the composite to fail in a catastrophic-like tensile fracture. The other composites showed an intermediate behaviour, closer to that observed for C-QI11.

Table 2
Main properties of composites

Composite	V_f	V_m	P	ILSS	FS
C-QI0	77.3	17.2	5.5	24.9	335
C-QI11	65.4	23.1	11.5	26.8	514
C-QI50	45.2	48.4	6.4	>35.9	–

V_f, volume fraction of fibres (vol.%); V_m, volume fraction of matrix (vol.%); d, bulk density (g cm^{-3}); P, porosity (vol.%); $P_{f/m}$, fibre/matrix debonding cracks (vol.%); ILSS, interlaminar shear strength (MPa); FS, flexural strength (MPa).

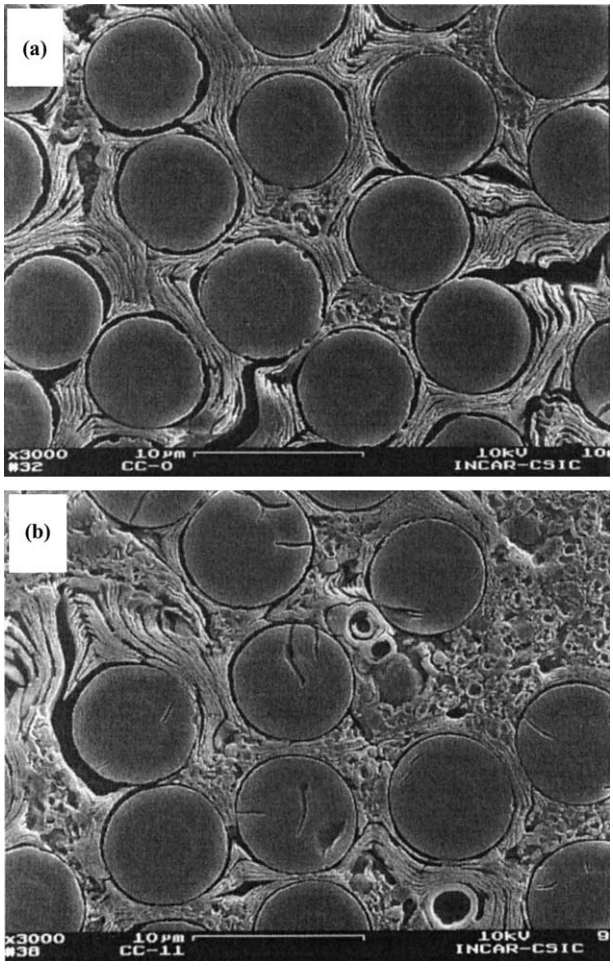

Fig. 5. SEM micrographs of composites: (a) C-QI0 and (b) C-QI11. The absence of QI in C-QI0 leads to the formation of microcracks at the fibre–matrix interface.

3.3. Effect of porosity

In addition to the fibre–matrix interface and the matrix texture, the porosity of the composite is a relevant parameter that should also be studied. The effect of porosity on the mechanical properties and fracture behaviour of the composites was studied in a series of composites submitted to several densification cycles. In the undensified composite, three types of voids are observed (Fig. 8a). These are elongated cracks between fibre bundles in both, lateral and transverse directions, and isolated devolatilization pores between or within bundles. Lateral cracks appear to be genuine cracks produced by matrix shrinkage during carbonisation and by the misalignment of fibres during the wet-winding step. Transverse cracks may be devolatilizaton pores joined together by cracks. As not all the voids in the undensified composites were intramatrix-located, the

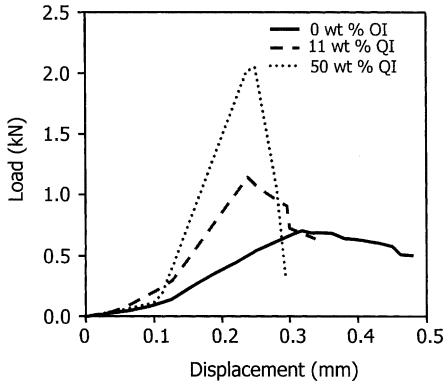

Fig. 6. Load–displacement curves of composites obtained from matrices with different quinoline insoluble contents. The presence of QI leads to an increase in the shear strength but this is accompanied by a brittle behaviour.

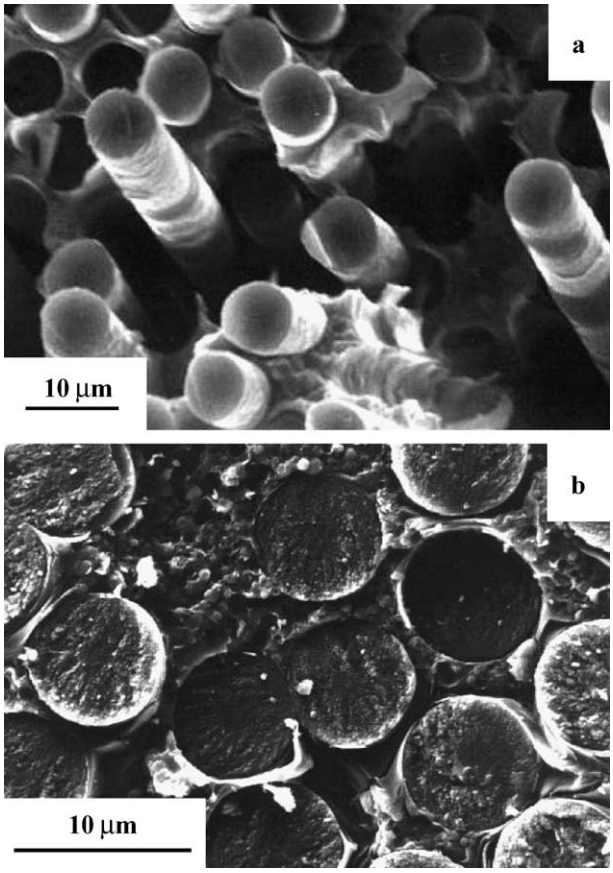

Fig. 7. SEM micrographs of fracture surfaces of composites: (a) C-QI0 and (b) C-QI11, showing fibre pull-out in the first one and a catastrophic fracture in the latter.

filling of the pores as densification proceeded affected the fibre–matrix interactions and therefore, it is expected to affect the composite mechanical behaviour. Fig. 8b and c show the filling of different pores on densification. In the case of Fig. 8b, a devolatilization pore partially filled with matrix on densification is observed,

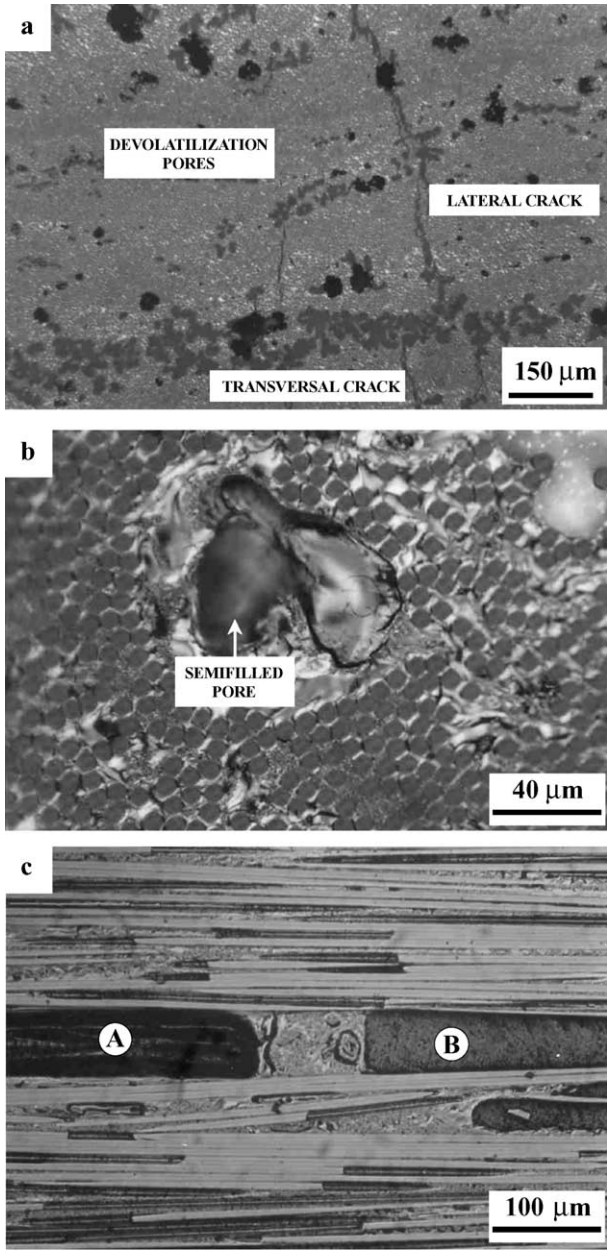

Fig. 8. Optical micrographs of composites: (a) C-DN0, (b) C-DN1 and (c) C-DN3, illustrating the evolution of different types of pores during densification. Position A corresponds to an unfilled pore and position B to the matrix precursor after densification but before recarbonisation.

while in Fig. 8c a longitudinal section of the composite shows a longitudinal pore showing the unfilled pore (position A) and the matrix precursor after densification but before recarbonisation (position B).

Generally speaking, densification caused the density of the composites to increase (Table 3), consequently, the open porosity decreased, which was accompanied by an increase in the composite strength. The interlaminar shear strength ranges between 16.4 and 34.3 MPa for the undensified composite and that obtained after five densification cycles, respectively.

Table 3
Main properties of composites with different densification cycles

Composite	V_m	d	P	ILSS
C-DN0	32.4	1.51	12.1	16.4
C-DN1	35.2	1.56	9.8	23.8
C-DN3P	39.3	1.66	5.7	25.2
C-DN5	42.2	1.68	2.8	34.4

V_m, volume fraction of matrix (vol.%); d, bulk density (g cm^{-3}); P, porosity (vol.%); ILSS, interlaminar shear strength (MPa).

Fig. 9 shows SEM images of the undensified composite (Fig. 9a) and the composite after five densification cycles (Fig. 9b and c). The filling of pores and also of debonding cracks on densification is clearly illustrated in these images. These results are in agreement with those obtained from the mechanical testing of the materials. As the number of densification cycles increased, the strength increases, but the material becomes more brittle in all cases. Fig. 10 illustrates the variation in the displacement/load curve with respect to the densification degree of the composite. In the curve corresponding to the composite after one densification cycle the elastic behaviour is not clearly defined. Before the maximum load is reached there are several losses of strength. Probably, some cracks are propagated through the matrix and then annulled at the interface or at a void.[15] After the maximum load is reached, the failure is progressive. This behaviour could be categorised as pseudo-plastic. However, after five densification cycles, a clear linear behaviour was observed up to the point of maximum load, which was then followed by a catastrophic failure. In these cases, the slope of the elastic zone is the greatest and consequently, the displacement associated with the maximum load is lower. It was found also that the behaviour of the composite with three densifications is an intermediate one.

For the interlaminar shear strength test, the slope of the linear zone depends on the properties of the matrix, the fibre and the debonding between the fibre and the matrix. Since the modulus of the fibres is higher than that of the matrix, even large variations in the matrix quantity (densifications) are expected to affect the modulus only slightly. It is supposed therefore that in the less densified composites greater porosity at the interface and matrix leads to a poor transfer of load to the fibres. In this situation the matrix controls the fracture mechanism. Hence, the value of the slope of the displacement–load curve is low and the behaviour pseudo-plastic. In the undensified porous matrix, cracks are easily initiated and propagate, spreading allowing the weak interface where they are blocked. In the more densified materials, the matrix bears greater loads without cracking. This together with a better interface (less porous) allows the fibre to play a major role in the mechanical test, causing an increase in the initial slope. At the same time modes of failure related with fibre breakage under tensile stress and catastrophic behaviour appear. This is in agreement with the fracture surfaces observed in these composites (Fig. 11), where composite C-DN0 shows debonding of fibre and matrix with significant fibre pull-out, while composite C-DN5 seems to have a more simultaneous failure of matrix and fibres with shorter pull-out lengths, thus indicating the existence of a stronger adhesion between matrix and fibre.

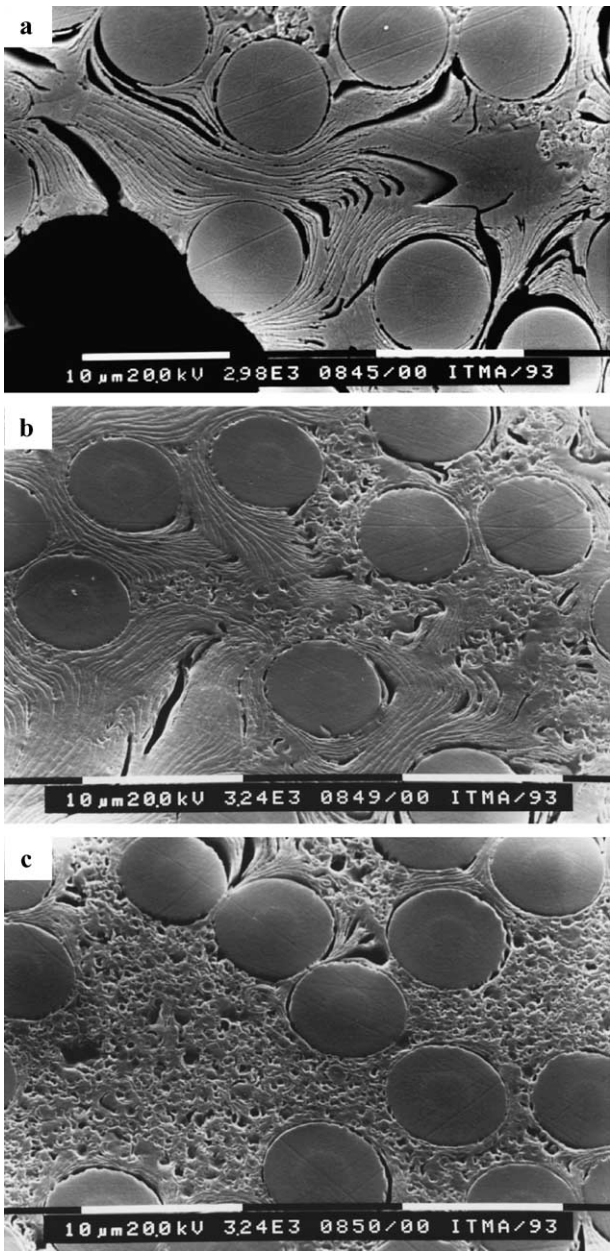

Fig. 9. SEM micrographs of composites: (a) C-DN0, (b) and (c) C-DN5, illustrating the filling of the pores and also of debonding cracks on densification.

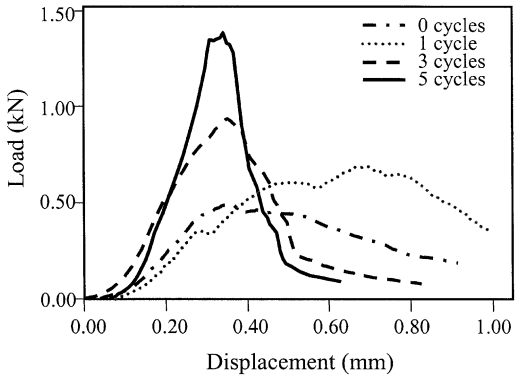

Fig. 10. Load–displacement curves of composites with different densification degrees. Densification of the composites caused the strength to increase but at the same time changed the failure mode from pseudo-plastic to brittle.

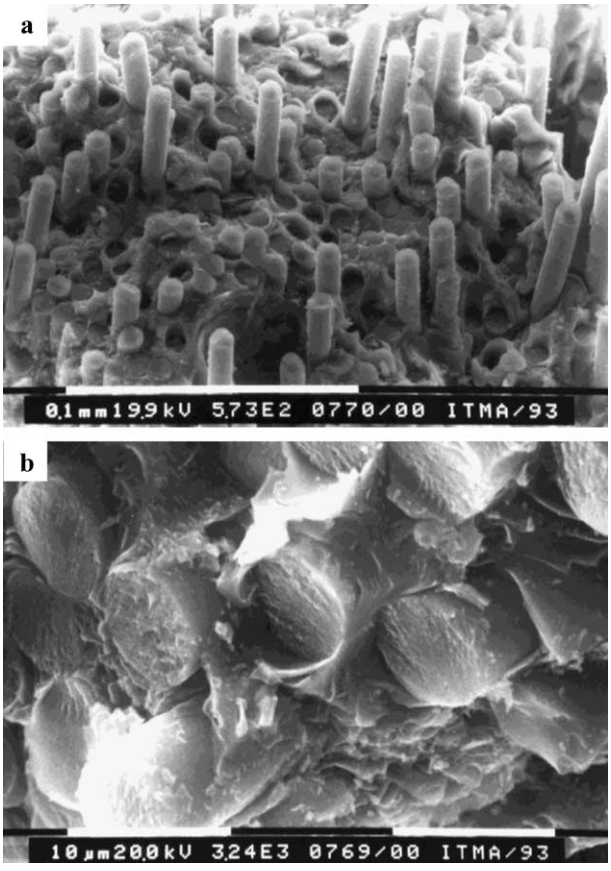

Fig. 11. SEM micrographs of fracture surfaces of composites: (a) C-DN0 and (b) C-DN5, illustrating fibre pull-out in the first sample and a more simultaneous failure of fibre and matrix for the latter.

4. Conclusions

The fracture behaviour of carbon–carbon composites is determined by the matrix texture and the fibre–matrix interface developed in the composite. In general, the presence of a mosaics-like texture of the matrix suggested a strong fibre–matrix interface and a denser microstructure, which made the materials to have higher interlaminar shear strength. On the other hand, composites with a matrix of domains seemed to have weaker interfaces resultant from shrinkage cracks at the interface. These materials had lower strength but showed a pseudo-plastic failure mode, caused by debonding of fibre and matrix during fracture. Significant fibre pull-out was observed at the fracture surface of these composites. In the same way, densification yielded stronger composites but changed the failure mode from pseudo-plastic to catastrophic, probably as a result of the better fibre–matrix interfaces developed and reduction in porosity. The fracture behaviour of carbon–carbon composites can be controlled by the proper selection of the pitch-based matrix precursor and processing conditions, as these will determine the matrix texture and thus the fibre matrix interface developed in the composite.

References

1. Fitzer, E., The future of carbon–carbon composites. *Carbon*, 1983, **25**, 163–190.
2. Savage, G., *Carbon–Carbon Composites*. Chapman and Hall, London, 1993.
3. Rand, B., Matrix precursors for carbon–carbon composite. In *Essentials of Carbon–Carbon Composites*, ed. C. R. Thomas. The Royal Society of Chemistry, Cambridge, 1993, pp. 67–102.
4. McEnaney, B. and Mays, T., Relationships between microstructure and mechanical properties in carbon–carbon composites. In *Essentials of Carbon–Carbon Composites*, ed. C. R. Thomas. The Royal Society of Chemistry, Cambridge, 1993, pp. 143–173.
5. Appleayard, S. P. and Rand, B., The effect of fibre–matrix interactions on the fabrication and structure of unidirectional carbon/carbon composites. *Carbon*, 2002, **40**, 817–834.
6. Figueiras, A., Fernéndez, J. J., Granda, M., Bermejo, J., Casal, E. and Menéndez, R., Influence of matrix precursors on the microstructure and mechanical properties of C/C composites. *Journal of Microscopy*, 1995, **177**, 218–229.
7. Ahearn, C. and Rand, B., Modification of the fibre–matrix bonding in a brittle carbon–carbon composite by controlled oxidation. *Carbon*, 1996, **34**, 239–249.
8. Figueiras, A., Granda, M., Casal, E., Bermejo, J., Bonhomme, J. and Menéndez, R., Influence of primary QI on pitch pyrolysis with reference to unidirectional C/C composites. *Carbon*, 1998, **36**, 883–891.
9. Casal, E., Granda, M., Bermejo, J. and Menéndez, R., Monitoring unidirectional carbon/carbon composite processing by light microscopy. *Journal of Microscopy*, 2001, **201**, 324–332.
10. Forrest, M. A. and Marsh, H., Coal and coal products: analytical characterisation techniques. In *American Chemical Society Symposium Series, vol. 205*, ed. Fuller Jr. American Chemical Society, Washington, DC, 1982.
11. Forrest, M. A. and Marsh, H., Structure in C–C fibre composites studied by microscopy and etching with chromic acid. *Journal of Materials Science*, 1983, **18**, 973–977.
12. White, J. L. and Zimmer, J. E., Mesophase alignment within carbon–fibre bundles. *Carbon*, 1983, **21**, 323–324.
13. Menéndez, R., Granda, M., Fernández, F. F., Figueiras, A., Bermejo, J., Bonhomme, J. and Belzunce, J., Influence of pitch air-blowing and thermal treatment on the microstructure and mechanical properties of carbon/carbon composites. *Journal of Microscopy*, 1997, **185**, 146–156.

14. Menéndez, R., Fernéndez, J. J., Bermejo, J., Cebolla, V., Mochida, I. and Korai, Y., The role of carbon black/coal-tar pitch interactions in the early stage of carbonization. *Carbon*, 1996, **34**, 895–902.

15. Casal, E., Granda, M., Bermejo, J., Bonhomme, J. and Menéndez, R., Influence of porosity on the apparent interlaminar shear strength of pitch-based unidirectional C–C composites. *Carbon*, 2001, **39**, 73–82.